Article

Optimal Selection and Integration of Batteries and Renewable Generators in DC Distribution Systems through a Mixed-Integer Convex Formulation

Jerson Daniel Basto-Gil [1] , Angel David Maldonado-Cardenas [1] and Oscar Danilo Montoya [1,2,*]

[1] Grupo de Compatibilidad e Interferencia Electromagnética, Facultad de Ingeniería, Universidad Distrital Francisco José de Caldas, Bogotá 110231, Colombia
[2] Laboratorio Inteligente de Energía, Facultad de Ingeniería, Universidad Tecnológica de Bolívar, Cartagena 131001, Colombia
[*] Correspondence: odmontoyag@udistrital.edu.co

Abstract: The problem concerning the optimal placement and sizing of renewable energy resources and battery energy storage systems in electrical DC distribution networks is addressed in this research by proposing a new mathematical formulation. The exact mixed-integer nonlinear programming (MINLP) model is transformed into a mixed-integer convex model using McCormick envelopes regarding the product between two positive variables. Convex theory allows ensuring that the global optimum is found due to the linear equivalent structure of the solution space and the quadratic structure of the objective function when all the binary variables are defined. Numerical results in the 21-bus system demonstrate the effectiveness and robustness of the proposed solution methodology when compared to the solution reached by solving the exact MINLP model. Numerical results showed that the simultaneous allocation of batteries and renewable energy resources allows for the best improvements in the daily operating costs, i.e., about 53.29% with respect to the benchmark case of the 21-bus grid, followed by the scenario where the renewable energy resources are reallocated while considering a fixed location for the batteries, with an improvement of 43.33%. In addition, the main result is that the difference between the exact modeling and the proposed formulation regarding the final objective function was less than 3.90% for all the simulation cases, which demonstrated the effectiveness of the proposed approach for operating distributed energy resources in monopolar DC networks.

Keywords: energy storage systems; mixed-integer convex model; renewable energy sources; convex optimization; McCormick envelopes

1. Introduction

In recent decades, the trend involving the use DC networks in distribution systems has increased significantly due to these networks' great compatibility with renewable energies, DC loads, and storage devices; in the same way that the investment costs of a DC network at medium voltage levels are much lower than those of an AC network and that its performance remains constant without being affected by the reactive power requirements of the load, unlike AC [1–3]. Global warming—and therefore the need to reduce fossil fuels—has triggered a search for renewable energies such as wind, solar, and tidal in order to mitigate the negative effects of greenhouse gas emissions to the atmosphere [1,4–6]. Direct current (DC) system technologies can be easily implemented in urban or rural areas, since they can be used in buildings and houses of different sizes. In addition, these distribution systems can be interconnected with the main power system, and they can operate independently [1].

When using renewable sources as the main energy supply, a set of issues comes to light: weather dependence, geographical location, and surface area. Among the most used

technologies are solar, wind, tidal, and geothermal, and each one of them has a different dependency on the primary energy resource [7]. For example, solar power depends on the solar radiation produced in the hours between dawn and sunset, which is usually 12 h. As for the wind, it uses turbines that depend on the speed of the wind, which is why they are located at a certain height. In addition, the average wind speed in the area of installation must be taken into account. This means that these technologies are not reliable in some areas with low wind speeds [8,9]. In light of the above, technologies such as battery energy storage systems (BESS) are used, and there are control strategies that can help maximize the power delivered by renewable sources, minimize harmonics, regulate voltage, and increase network efficiency, as can be consulted in [10,11]. This helps reduce the intermittency of renewable sources. The use of BESS enhances the reliability and quality of the energy supply service [12–14].

By using BESS, the disadvantages mentioned above are undermined. This is done by storing energy within them at times of low demand and supplying it at times of high demand [15,16]. By making use of batteries within a DC distribution system, energy generation costs can be reduced. This is done by optimally locating BESS within the network through different optimization methods. This can be observed in [17], where the authors proposed particle swarm optimization while using a 30-node IEEE system as an example. They determined the optimal location of the BESS by locating the renewable source (i.e., wind sources) in different nodes of the system. Moreover, while establishing the optimal location of the BESS, they found important information about the generation costs of the nodes. In [18], the authors determined the optimal location of the BESS by formulating a mixed non-integer nonlinear programming (MINLP) model, which was transformed into a convex mixed-integer quadratic equivalent (MIQC) in order to obtain a global optimum instead of a local one. These models were solved via the General Algebraic Modeling System (GAMS) software. The error in the objective function between the MINLP and the proposed model was 4%. To solve these models, the BONMIN solver was used, through which the MINLP model showed an improvement of 10.85% with respect to the base case. However, the MIQC achieved an improvement of 18.55%. This result demonstrated the efficiency of the MIQC model when locating BESS with respect to the exact non-convex formulation (i.e., the MINLP formulation). In [19], the authors proposed a convex quadratic model that allows identifying the best nodes in which the renewable sources can be located within a DC network. In addition, to locate the sources in these nodes, the authors also determined the capacity necessary to achieve optimal results. However, in this research, the authors did not include daily load curves or BESS, which reduces the applicability of their proposal in real DC networks.

Other authors have addressed the problem regarding the optimal placement and sizing of dispersed generators and BESS with different mathematical and combinatorial optimizers. Some of these are the application of the whale optimization algorithm to locate BESS in distribution networks [20], the application of a mixed-integer conic formulation to locate and size BESS and DGs in distribution networks via piece-wise linearization of the power losses [21], the implementation of parallel particle swarm optimization to define the optimal daily operation of BESS in radial DC networks [22], the optimal operation of BESS in DC networks using semi-definite programming [23], and artificial neural networks to determine the size of BESS while considering loss sensitive analysis for microgrids [24].

Considering the aforementioned studies, the main contributions of this research are:

i. The simultaneous integration of BESS and dispersed generators in monopolar DC networks, since this problem is typically addressed independently by integrating only one of these devices into the DC grid, or both in a sequential fashion, i.e., in the first stage, the dispersed sources are assigned, and batteries are integrated in the second stage.

ii. The reformulation of the exact MINLP model that represents the optimal placement and sizing of BESS and DG into a mixed-integer convex (MIC) formulation via the

application of McCormick envelopes to approximate the product between two continuous variables through a linear equivalent restriction.

This is the procedure followed to compare the exact MINLP model with the proposed MIC formulation: (i) the MINLP model is solved using the BONMIN solver in the GAMS software, (ii) the proposed MIC model is solved using the convex disciplined tool for MATLAB software called CVX with the Gurobi solver; (iii) the optimal sizes of the dispersed generators and batteries provided with the solution of the MIC model are evaluated in the MINLP model in GAMS in order to eliminate the error introduced during the application of McCormick envelopes to approximate the power balance constraint.

Note that our contribution supposes that the irradiance for PV generation and the wind speed remain as constant inputs in the proposed optimization models. This is supported by the fact that the monopolar DC network covers an area of a few hundred square meters, which implies that the variability of the renewable energy resources can be neglected. However, in future works, it will be necessary to conduct studies where partial shading or wind speed variations are directly included in the optimization model.

2. Mathematical Representation

To select and locate the BESS, together with determining the optimal location of renewable sources in DC distribution networks, a mixed-integer nonlinear programming formulation is used which considers the high penetration of renewable sources and can be represented through multi-period economic dispatch formulation. The nonlinear component of the model comprises the products between voltage variables in the power balance constraints, and the binary part corresponds to the variables regarding the location of the renewable energy resources and batteries.

2.1. Objective Function

This section presents the objective function of the exact model for the optimal location and selection of BESS and renewable sources in a DC distribution system, which consists of minimizing the costs of energy losses for a daily operation scenario. This function is defined in Equation (1).

$$\min f_1 = CoE \sum_{t \in \mathcal{H}} \sum_{i \in \mathcal{B}} v_{i,t} \left(\sum_{j \in \mathcal{B}} G_{ij} v_{j,t} \right) \Delta_t \tag{1}$$

The objective function is defined as f_1, which is related to the daily cost of the energy losses, where CoE is the average energy cost of the energy in the electricity market, $v_{i,t}$ and $v_{j,t}$ are the voltage values at nodes i and j for each period of time t, G_{ij} represents the conductive effect that relates nodes i and j and is contained in the conductance matrix of the DC network, and Δ_t defines the variation of the period of time (typically 1 h for daily operation). Note that $\mathcal{B}$ and $\mathcal{H}$ define the sets that contain all the nodes of the monopolar DC network and the number of periods of study, respectively.

f_1	Value of the objective function regarding the cost of the daily energy losses (COP\$/day).
CoE	Average energy cost of the energy in the electricity market (COP\$/Wh-day).
$v_{i,t}$	Voltage value at node i for each period of time t (V).
$v_{j,t}$	Voltage value at node j for each period of time t (V).
G_{ij}	Conductive effect that relates nodes i and j (S).
Δ_t	Variation of the period of time where electrical variables are assumed as constants (h).
$\mathcal{H}$	Set that contains all the number of periods of study.
$\mathcal{B}$	Set that contains all the nodes of the monopolar DC network.

2.2. Mathematical Formulation for including Batteries

For this model, Equation (1) is used as the objective function. Moreover, this model includes the following set of constraints:

$$p_{i,t} + p_{i,t}^{dg} + \sum_{b\in\mathcal{E}} p_{i,t}^b - p_{i,t}^d = v_{i,t} \sum_{j\in\mathcal{B}} G_{ij} v_{j,t}, \ \{\forall i \in \mathcal{B} \ \forall t \in \mathcal{H}\} \tag{2}$$

$$SoC_{i,t}^b = SoC_{i,t-1}^b - \varphi_i^b p_{i,t}^b \Delta_t, \ \{\forall b \in \mathcal{E}, \ \forall i \in \mathcal{B}, \ \forall t \in \mathcal{H}\} \tag{3}$$

$$SoC_{i,t_0}^b = x_i^b SoC_i^{b,\text{ini}}, \ \{\forall b \in \mathcal{E}, \ \forall i \in \mathcal{B}\} \tag{4}$$

$$SoC_{i,t_f}^b = x_i^b SoC_i^{b,\text{fin}}, \ \{\forall b \in \mathcal{E}, \ \forall i \in \mathcal{B}\} \tag{5}$$

$$p_{i,t}^{\min} \le p_{i,t} \le p_{i,t}^{\max}, \ \{\forall i \in \mathcal{B}, \ \forall t \in \mathcal{H}\} \tag{6}$$

$$p_{i,t}^{dg,\min} \le p_{i,t}^{dg} \le p_{i,t}^{dg,\max}, \ \{\forall i \in \mathcal{B}, \ \forall t \in \mathcal{H}\} \tag{7}$$

$$x_i^b p_i^{b,\min} \le p_{i,t}^b \le x_i^b p_i^{b,\max}, \ \{\forall b \in \mathcal{E}, \ \forall i \in \mathcal{B}, \ \forall t \in \mathcal{H}\} \tag{8}$$

$$v_i^{\min} \le v_{i,t} \le v_i^{\max}, \ \{\forall i \in \mathcal{B}, \ \forall t \in \mathcal{H}\} \tag{9}$$

$$x_i^b SoC_i^{b,\min} \le SoC_{i,t}^b \le x_i^b SoC_i^{b,\max}, \ \{\forall b \in \mathcal{E}, \ \forall i \in \mathcal{B}, \ \forall t \in \mathcal{H}\} \tag{10}$$

$$\sum_{b\in\mathcal{E}} \sum_{i\in\mathcal{B}} x_i^b = N_b^{\max} \tag{11}$$

where $p_{i,t}$ represents the power generation in the slack source and $p_{i,t}^{dg}$ the power injection in the renewable energy resource; $p_{i,t}^b$ corresponds to the active power injected/absorbed by the BESS connected at node i in period of time t; parameter $p_{i,t}^d$ represents the power consumption at node i in the period of time t; $SoC_{i,t}^b$ is the state of charge of the BESS; φ_i^b represents the battery charge/discharge coefficient; x_i^b is a binary variable that defines whether a BESS is connected at node i or not; $SoC_i^{b,ini}$ and $SoC_i^{b,fin}$ are the initial and final states of charge of the BESS connected at node i; $p_{i,t}^{\min}$ and $p_{i,t}^{\max}$ correspond to the minimum and maximum power bounds allowed for generation in the slack source; $p_{i,t}^{dg,\min}$ and $p_{i,t}^{dg,\max}$ are the lower and upper power injection limits of the renewable energy sources; $p_i^{b,\min}$ and $p_i^{b,\max}$ are the nominal capabilities of power absorption/injection in the BESS; $v_i^{\min}$ and $v_i^{\max}$ represent the minimum and maximum voltage regulation limits allowed for all the nodes in the network; $SoC_i^{b,\min}$ and $SoC_i^{b,\max}$ are the lower and upper state-of-charge bounds for the BESS; and $N_b^{\max}$ represents the maximum number of BESS available for integration in a monopolar DC network. Note that $\mathcal{E}$ is the set that contains all the BESS technologies available.

$p_{i,t}$	Power generation in the slack source connected at node i in the period of time t (W).
$p_{i,t}^{dg}$	Power generation in the distributed generator connected at node i in the period of time t (W).
$p_{i,t}^b$	Power generation/absorption in the BESS connected at node i in the period of time t (W).
$p_{i,t}^d$	Power demand at node i in the period of time t (W).
$SoC_{i,t}^b$	State of charge of the BESS at node i in the period of time t (%).
φ_i^b	Battery charge/discharge coefficient (%/Wh).
x_i^b	Binary variable that defines whether a BESS is connected at node i or not.
$SoC_i^{b,ini}$	Initial state of charge of the BESS at node i (%).
$SoC_i^{b,fin}$	Final state of charge of the BESS at node i (%).
$p_{i,t}^{\min}$	Minimum power generation in the slack source connected at node i in the period of time t (W).

$p_{i,t}^{\max}$	Maximum power generation in the slack source connected at node i in the period of time t (W).
$p_{i,t}^{dg,\min}$	Minimum power generation in the distributed generator connected at node i in the period of time t (W).
$p_{i,t}^{dg,\max}$	Maximum power generation in the distributed generator connected at node i in the period of time t (W).
$p_{i,t}^{b,\min}$	Minimum power bound allowed for the BESS system at node i in the period of time t (W).
$p_{i,t}^{b,\max}$	Maximum power bound allowed for the BESS system at node i in the period of time t (W).
$v_i^{\min}$	Minimum voltage regulation limit allowed for all the nodes in the network (V).
$v_i^{\max}$	Maximum voltage regulation limit allowed for all the nodes in the network (V).
$SoC_i^{b,\min}$	Lower state-of-charge bound for the BESS connected at node i (%).
$SoC_i^{b,\max}$	Upper state-of-charge bound for the BESS connected at node i (%).
$N_b^{\max}$	Maximum number of BESS available for integration in a monopolar DC network.
$\mathcal{E}$	Set that contains all the BESS technologies available.

2.3. Formulation for the Optimal Placement of Renewable Energy Sources

This optimization model also considers the same objective function as the previous one, i.e., the minimization of the total energy losses costs. The complete set of constraints for this model is presented below:

$$p_{i,t} + p_{i,t}^w + p_{i,t}^{pv} + \sum_{b \in \mathcal{E}} p_{i,t}^b - p_{i,t}^d = v_{i,t} \sum_{j \in \mathcal{B}} G_{ij} v_{j,t}, \; \{\forall i \in \mathcal{B} \; \forall t \in \mathcal{H}\} \tag{12}$$

$$SoC_{i,t}^b = SoC_{i,t-1}^b - \varphi_i^b p_{i,t}^b \Delta_t, \; \{\forall b \in \mathcal{E}, \; \forall i \in \mathcal{B}, \; \forall t \in \mathcal{H}\} \tag{13}$$

$$SoC_{i,t_0}^b = SoC_i^{b,\text{ini}}, \; \{\forall b \in \mathcal{E}, \; \forall i \in \mathcal{B}\} \tag{14}$$

$$SoC_{i,t_f}^b = SoC_i^{b,\text{fin}}, \; \{\forall b \in \mathcal{E}, \; \forall i \in \mathcal{B}\} \tag{15}$$

$$p_{i,t}^{\min} \leq p_{i,t} \leq p_{i,t}^{\max}, \; \{\forall i \in \mathcal{B}, \; \forall t \in \mathcal{H}\} \tag{16}$$

$$x_i^w p_{i,t}^{w,\min} \leq p_{i,t}^w \leq x_i^w p_{i,t}^{w,\max}, \; \{\forall i \in \mathcal{B}, \; \forall t \in \mathcal{H}\} \tag{17}$$

$$x_i^{pv} p_{i,t}^{pv,\min} \leq p_{i,t}^{pv} \leq x_i^{pv} p_{i,t}^{pv,\max}, \; \{\forall i \in \mathcal{B}, \; \forall t \in \mathcal{H}\} \tag{18}$$

$$p_i^{b,\min} \leq p_{i,t}^b \leq p_i^{b,\max}, \; \{\forall b \in \mathcal{E}, \; \forall i \in \mathcal{B}, \; \forall t \in \mathcal{H}\} \tag{19}$$

$$v_i^{\min} \leq v_{i,t} \leq v_i^{\max}, \; \{\forall i \in \mathcal{B}, \; \forall t \in \mathcal{H}\} \tag{20}$$

$$SoC_i^{b,\min} \leq SoC_{i,t}^b \leq SoC_i^{b,\max}, \; \{\forall b \in \mathcal{E}, \; \forall i \in \mathcal{B}, \; \forall t \in \mathcal{H}\} \tag{21}$$

$$\sum_{i \in \mathcal{B}} x_i^w = N_w^{\max} \tag{22}$$

$$\sum_{i \in \mathcal{B}} x_i^{pv} = N_{pv}^{\max}. \tag{23}$$

Unlike the one defined in Equations (1)–(11), in this optimization model, the binary variable x_i^b is set as 1 in the nodes where these BESS will be assigned. Moreover, there are two new binary variables regarding the optimal integration of renewable generators based on photovoltaic and wind technologies, i.e., x_i^{pv} and x_i^w. In addition to these variables, the power injection in both sources is represented by means of $p_{i,t}^{pv}$ and $p_{i,t}^w$, which includes their minimum and maximum generation bounds $p_{i,t}^{pv,\min}$, $p_{i,t}^{pv,\max}$, $p_{i,t}^{w,\min}$, and $p_{i,t}^{w,\max}$, respectively. $N_{pv}^{\max}$ and $N_w^{\max}$ represent the maximum number of distributed generators available for integration in a monopolar DC network.

x_i^{pv}	Binary variable that defines whether a PV source is connected at node i or not.
x_i^{w}	Binary variable that defines whether a wind source is connected at node i or not.
$p_{i,t}^{pv}$	Power generation in the PV source connected at node i in the period of time t (W).
$p_{i,t}^{w}$	Power generation in the wind source connected at node i in the period of time t (W).
$p_{i,t}^{pv,\min}$	Minimum power generation in the PV source connected at node i in the period of time t (W).
$p_{i,t}^{dg,\max}$	Maximum power generation in the PV source connected at node i in the period of time t (W).
$p_{i,t}^{w,\min}$	Minimum power generation in the wind source connected at node i in the period of time t (W).
$p_{i,t}^{w,\max}$	Maximum power generation in the wind source connected at node i in the period of time t (W).
$N_{pv}^{\max}$	Maximum number of PV sources available for integration in a monopolar DC network.
$N_{w}^{\max}$	Maximum number of wind sources available for integration in a monopolar DC network.

2.4. Interpretation of the Optimization Models

The general mathematical formulation given from Equations (1)–(23) represents the exact MINLP formulation for two problems. The first problem corresponds to the optimal selection and location of BESS in monopolar DC networks, whereas the second model defines the optimal siting and sizing of renewable generation sources in monopolar DC networks.

2.4.1. BESS Model Interpretation

In this optimization problem, Equation (1) corresponds to the formulation of the objective function, which is entrusted with defining the total grid energy losses costs for a daily operation scenario; Equation (2) corresponds to the power equilibrium constraint at each node of the network for each period of time; Equation (3) defines the linear behavior of the state of charge of the BESS; Equations (4) and (5) represent the initial and final desired states of charge of the BESS; inequality constraints Equations (6)–(8) define the upper and lower bounds for power generation in the slack source, the renewable energy resources, and the BESS, respectively; inequality constraint Equation (9) is known as the voltage regulation constraint, which corresponds to physical bounds for the voltage magnitudes in all nodes of the network in order to ensure the correct operation of all the devices connected to it; and inequality constraints Equations (10) and (11) define the lower and upper operation bounds for the BESS integrated into the monopolar DC network and the maximum number of batteries that can be installed on the grid, respectively.

2.4.2. Renewable Energy Model Interpretation

In the case of the optimization model for optimal integration of renewable energy systems in a monopolar DC network, the minimization of daily energy losses costs is considered as the objective function, as defined in Equation (1). In addition, the power equilibrium is defined via Equation (12). Equation (13) defines the linear behavior of the state of charge for the batteries connected across the DC network. Equations (4) and (5) represent the initial and final desired states of charge of the BESS. The set of inequality constraints (16)–(19) defines the minimum and maximum power injection bounds in the slack source, the renewable energy resources, and the BESS, respectively. Inequality constraints Equations (20) and (21) have the same interpretation as Equations (9) and (10), respectively. Finally, inequality constraints Equations (22) and (23) define the maximum number for photovoltaic and wind generation sources that can be integrated into the monopolar DC network, respectively.

3. Proposed MIC Reformulation

Mathematical Formulations (1)–(11), (1), and (12)–(23) constitute a general MINLP formulation to integrate BESS and renewable energy sources in monopolar DC networks, even if the objective function is convex, since the conductance matrix G is positive semi-definite and most of the equations are linear or linear-integer. However, the nonlinearity of these models lies in the power equilibrium constraints, i.e., Equations (2) and (12), specifically in the product between the voltage variables on their right-hand side [25].

Note that, in order to obtain an equivalent MIC formulation that represents the exact MINLP models for the studied problems, the McCormick equivalent of the product between two positive variables is employed as initially presented in [19]. To illustrate the equivalent representation of the product of two positive variables, consider Equation (24):

$$f(w_1, w_2) = w_1 w_2. \tag{24}$$

Now, if we apply Taylor's series expansion around the linearizing point (w_{10}, w_{20}), the following general expansion of the product between two variables is obtained [18]:

$$f(w_1, w_2) = w_{20} w_1 + w_{10} w_2 + w_{10} w_{20} + f_{H.O.T}(w_1, w_2, w_{10}, w_{20}), \tag{25}$$

where $f_{H.O.T}(w_1, w_2, w_{10}, w_{20})$ are known as the high-order-terms of the Taylor's series expansion. Note that these terms can be neglected for power flow analysis, since the voltage magnitudes exhibit small variations around the 1.0 value when a per-unit representation is used [18]. Now, by changing the generic variables w_1 and w_2 for the voltage variables $v_{i,t}$ and $v_{j,t}$, the linear equivalent constraint associated with the power balance at each node of the network for both optimization models is obtained.

$$p_{i,t} + p_{i,t}^{dg} + \sum_{b \in \mathcal{E}} p_{i,t}^b - p_{i,t}^d = \sum_{j \in \mathcal{B}} G_{ij}(v_{i,t}v_{j0,t} + v_{i0,t}v_{j,t} - v_{i0,t}v_{j0,t}), \ \{\forall i \in \mathcal{B} \ \forall t \in \mathcal{H}\} \tag{26}$$

$$p_{i,t} + p_{i,t}^w + p_{i,t}^{pv} + \sum_{b \in \mathcal{E}} p_{i,t}^b - p_{i,t}^d = \sum_{j \in \mathcal{B}} G_{ij}(v_{i,t}v_{j0,t} + v_{i0,t}v_{j,t} - v_{i0,t}v_{j0,t}), \ \begin{Bmatrix} \forall i \in \mathcal{B} \\ \forall t \in \mathcal{H} \end{Bmatrix} \tag{27}$$

$f(w_1, w_2)$ General nonlinear function of two variables.
w_1 Auxiliary variable number 1.
w_2 Auxiliary variable number 2.
w_{10} Initial value of the auxiliary variable number 1.
w_{20} Initial value of the auxiliary variable number 2.
$f_{H.O.T}(\cdot)$ High-order terms of the Taylor series expansion for a general nonlinear function.
$v_{i0,t}$ Initial voltage value at node i for each period of time t (V).
$v_{j0,t}$ Initial voltage value at node j for each period of time t (V).

Remark 1. *Once the power balance constraint for each optimization model has been linearized using the McCormick equivalent, the MIC models for both studied problems take the following form:*

i. *The MIC model to select and locate BESS in monopolar DC networks is defined by Equation (1) and the set of constraints Equations (3)–(11), as well as by the linear equivalent power flow Equation (26).*

ii. *The MIC model to place and size renewable energy resources in monopolar DC networks is defined by Equation (1) and the set of constraints Equations (12)–(23), as well as by the linear equivalent power flow Equation (27).*

4. Solution Methodology

The objective of this research is to propose a general solution methodology for simultaneously integrating BESS and renewable energy resources in monopolar DC networks. To this effect, an algorithm is proposed which solves the mixed-integer models at the same time by setting the location of the renewable energy sources for the BESS model and

the renewable generation one. The proposed algorithmic implementation is presented in Algorithm 1.

Algorithm 1 Simultaneous allocation of BESS and renewable energy sources in monopolar DC networks using MIC models and recursive programming.

Data: Define the monopolar DC network under analysis
Select the average renewable energy availability curves;
Define the per-unit equivalent of the network;
Implement the optimization model for BESS in the CVX environment from
　MATLAB using the Gurobi solver;
Set the location of the renewable energy sources into the BESS model;
Solve the optimization model for BESS;
for $l = 1 : L_{\max}$ **do**
　Set these BESS in the optimization model for locating and sizing renewable
　　energy sources;
　Implement the optimization model for renewable energy sources in the CVX
　　environment from MATLAB using the Gurobi solver;
　Solve the optimization model for renewable energy sources;
　Implement the optimization model for BESS in the CVX environment from
　　MATLAB using the Gurobi solver;
　Set the location of the renewable energy sources into the BESS model;
　Solve the optimization model for BESS;
　if *Did the location of the BESS change?* **then**
　　Continue with the searching process;
　else
　　Report the final solution for the BESS and the renewable energy sources;
　　break;
　end
end
Result: Present the optimal solution for the BESS and the renewable energy
　　　　sources

Note that the recursive implementation in Algorithm 1 allows for the simultaneous allocation of BESS and renewable energy sources in monopolar DC networks using convex programming, which ensures that the global optimum is found for each optimization model [26,27]. Note that this algorithmic solution corresponds to the main contribution of this research.

5. Monopolar DC Network under Study

To validate the effectiveness of the proposed MIC models in the optimal integration of distributed energy resources for monopolar DC networks, the 21-bus system was employed. This system was originally proposed by [28] to analyze the convergence of the Newton–Raphson power flow method in DC grids. All the electrical parameters of the 21-bus grid, i.e., the resistances of the distribution lines, and the power consumption during peak hours were taken from [18] and are listed in Table 1. In addition, the electrical configuration of this distribution grid is presented in Figure 1.

To evaluate the daily energy performance, Table 2 presents the values for the demand and energy costs, considering that Δt is defined as a half-hour, which produces 48 values.

Table 1. Parametric information of the 21-bus grid (the power and voltage bases are 1 kV and 100 kW).

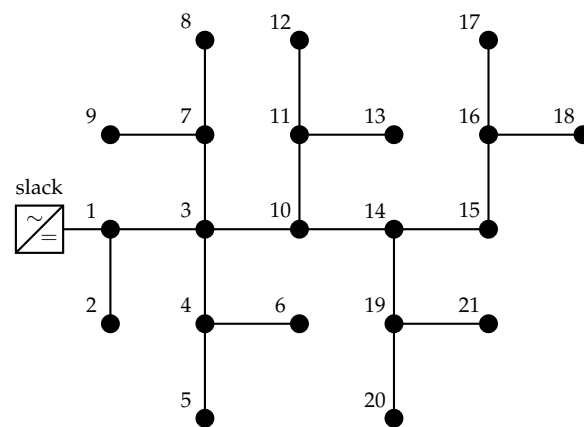| Node i	Node j	R_{ij} (pu)	P_j (pu)	Node i	Node j	R_{ij} (pu)	P_j (pu)
1 (slack)	2	0.0053	0.70	11	12	0.0079	0.68
1	3	0.0054	0.00	11	13	0.0078	0.10
3	4	0.0054	0.36	10	14	0.0083	0.00
4	5	0.0063	0.04	14	15	0.0065	0.20
4	6	0.0051	0.036	15	16	0.0064	0.23
3	7	0.0037	0.00	16	17	0.0074	0.43
7	8	0.0079	0.32	16	18	0.0081	0.34
7	9	0.0072	0.80	14	19	0.0078	0.09
3	10	0.0053	0.00	19	20	0.0084	0.21
10	11	0.0038	0.45	19	21	0.0081	0.21

Figure 1. Grid configuration of the 21-bus system.

Table 2. Demand and energy cost variations for a typical day of operation.

Time (h)	CoE (pu)	Dem. (%)	Time (h)	CoE (pu)	Dem. (%)	Time (h)	CoE (pu)	Dem. (%)
0.5	0.8105	34	8.5	0.9263	62	16.5	0.9737	90
1.0	0.7789	28	9.0	0.9421	68	17.0	1	90
1.5	0.7474	22	9.5	0.9579	72	17.5	0.9947	90
2.0	0.7368	22	10.0	0.9579	78	18.0	0.9895	90
2.5	0.7263	22	10.5	0.9579	84	18.5	0.9737	86
3.0	0.7316	20	11.0	0.9579	86	19.0	0.9579	84
3.5	0.7368	18	11.5	0.9579	90	19.5	0.9526	92
4.0	0.7474	18	12.0	0.9526	92	20.0	0.9474	100
4.5	0.7579	18	12.5	0.9474	94	20.5	0.9211	98
5.0	0.8000	20	13.0	0.9474	94	21.0	0.8947	94
5.5	0.8421	22	13.5	0.9421	90	21.5	0.8684	90
6.0	0.8789	26	14.0	0.9368	84	22.0	0.8421	84
6.5	0.9158	28	14.5	0.9421	86	22.5	0.7947	76
7.0	0.9368	34	15.0	0.9474	90	23.0	0.7474	68
7.5	0.9579	40	15.5	0.9474	90	23.5	0.7211	58
8.0	0.9421	50	16.0	0.9474	90	24.0	0.6947	50

Note that the value of the energy costs is set as COP\$/kWh 479.3389, just as in [18] for the same test feeder.

The electrical information of the BESS that can be integrated into the 21-bus grid is reported in Table 3. The batteries are classified using letters A and B according to the expected charging/discharging rates while considering nominal operation. Note that the initial location of these batteries was also taken from [18].

Table 3. BESS information.

Node	Type	ϕ^b	$p^{b,\max}$	$p^{b,\min}$
7	A	0.0625	4	-3.2
10	B	0.0813	3.2	-2.4616
15	B	0.0813	3.2	-2.4616

For this test feeder, the existence of two renewable energy resources was considered: one of them with wind technology and the other one with photovoltaic generation. The nominal sizes of these renewable generators is presented in Table 4, along with their initial locations. Their expected daily behavior is listed in Table 5.

Table 4. Nominal sizes of the renewable energy sources.

Node	Type	$P_{\max}$ (pu)	$P_{\min}$ (pu)
12	Wind	2.2152	0
21	Photovoltaic	2.8158	0

Table 5. Daily behavior of the renewable energy resources.

Period (h)	P_w (pu)	P_{pv} (pu)	Period (h)	P_w (pu)	P_{pv} (pu)	Period (h)	P_w (pu)	P_{pv} (pu)
0.5	0.6303	0	8.5	0.8271	0.0403	16.5	0.9892	0.4193
1.0	0.6194	0	9.0	0.8523	0.1344	17.0	0.9652	0.2784
1.5	0.6098	0	9.5	0.8788	0.2710	17.5	0.9244	0.1373
2.0	0.6050	0	10.0	0.9064	0.3673	18.0	0.8607	0.0374
2.5	0.6122	0	10.5	0.9328	0.4584	18.5	0.7743	0.0007
3.0	0.6411	0	11.0	0.9520	0.6125	19.0	0.7251	0
3.5	0.6927	0	11.5	0.9640	0.8134	19.5	0.7167	0
4.0	0.7395	0	12.0	0.9700	0.9122	20.0	0.7167	0
4.5	0.7779	0	12.5	0.9748	0.9633	20.5	0.7251	0
5.0	0.7887	0	13.0	0.9784	1.0000	21.0	0.7263	0
5.5	0.7671	0	13.5	0.9832	0.9582	21.5	0.7179	0
6.0	0.7479	0	14.0	0.9880	0.8791	22.0	0.7095	0
6.5	0.7287	0	14.5	0.9940	0.7308	22.5	0.6987	0
7.0	0.7371	0	15.0	0.9988	0.7645	23.0	0.6915	0
7.5	0.7731	0	15.5	1.0000	0.6866	23.5	0.6867	0
8.0	0.8031	0.0016	16.0	0.9964	0.5893	24.0	0.6831	0

6. Numerical Implementation and Results

The implementation of the MIC model was prepared and executed on a desktop computer with an AMD Ryzen 5 3600 6-Core 3.56 GHz processor and 16 GB RAM running a 64-bit version of Windows 10. The Matlab R2021b software was used with Gurobi version 9.5.1. The exact MINLP model was solved using the General Algebraic Modeling System (GAMS) software (GAMS Development Corp., Fairfax, VA, USA) (version 23.5) and the BONMIN solver.

Remark 2. *The operation of the batteries for all scenarios was set while considering that these BESS will have maintained 50% of their energy stored at the beginning and the end of a day.*

To validate the proposed recursive convex model to locate and size distributed energy resources in monopolar DC networks, four simulation cases were considered as presented below.

- Case 1: The initial locations of the BESS and renewable energy sources are maintained as indicated in Tables 3 and 4. The exact MINLP model and the MIC approximation

are evaluated with the binary variables fixed. These solutions provide the reference cases for both models.

- Case 2: This simulation case employs the proposed MIC model to find the optimal location of the BESS. These locations are set in the exact MINLP model in order to determine the exact value of the objective function.
- Case 3: This simulation case employs the proposed MIC model to optimally allocate the renewable energy resources. These locations are set in the exact MINLP model in order to determine the exact value of the objective function.
- Case 4: The simultaneous location of the BESS and the renewable energy sources is found via the recursive implementation in Algorithm 1. These locations are set in the exact MINLP model in order to determine the exact value of the objective function.

These cases were proposed to assess the efficiency of the integer-mixed convex model when locating BESS and renewable sources. The results were compared while regarding each problem as independent and considering the BESS and renewable sources to be simultaneously located.

6.1. Numerical Results for Case 1

This simulation scenario provides the reference case for the proposed MIC model and the exact MINLP formulation when the original location of the BESS and renewable sources are maintained (Tables 3 and 4). The electrical behavior of the BESS for this simulation case is presented in Figure 2.

It can be seen in Figure 2 that the deviations between the convex and the exact models are minimal. Also note that the state of charge and discharge of each battery starts and ends at 50% and the maximum charge value between the three batteries is 77.2%, while the lowest value observed is 49.1%. The batteries at nodes 10 and 15 are charged until period 34, after which the stored energy is supplied to the network, while the battery located at node 7 is charged until period 17, after which it delivers energy to the network. These variations show that the batteries depend on the energy demand connected to the distribution network.

Table 6 presents the optimal solutions obtained with the proposed MIC model and the MINLP one. When comparing our proposal with the MINLP model, the estimation error is about 3.90%, which is indeed a minimum error, taking into account that the MIC model is the first approximation of the exact MINLP model [18].

Table 6. Numerical results for the MIC and MINLP models in Case 1.

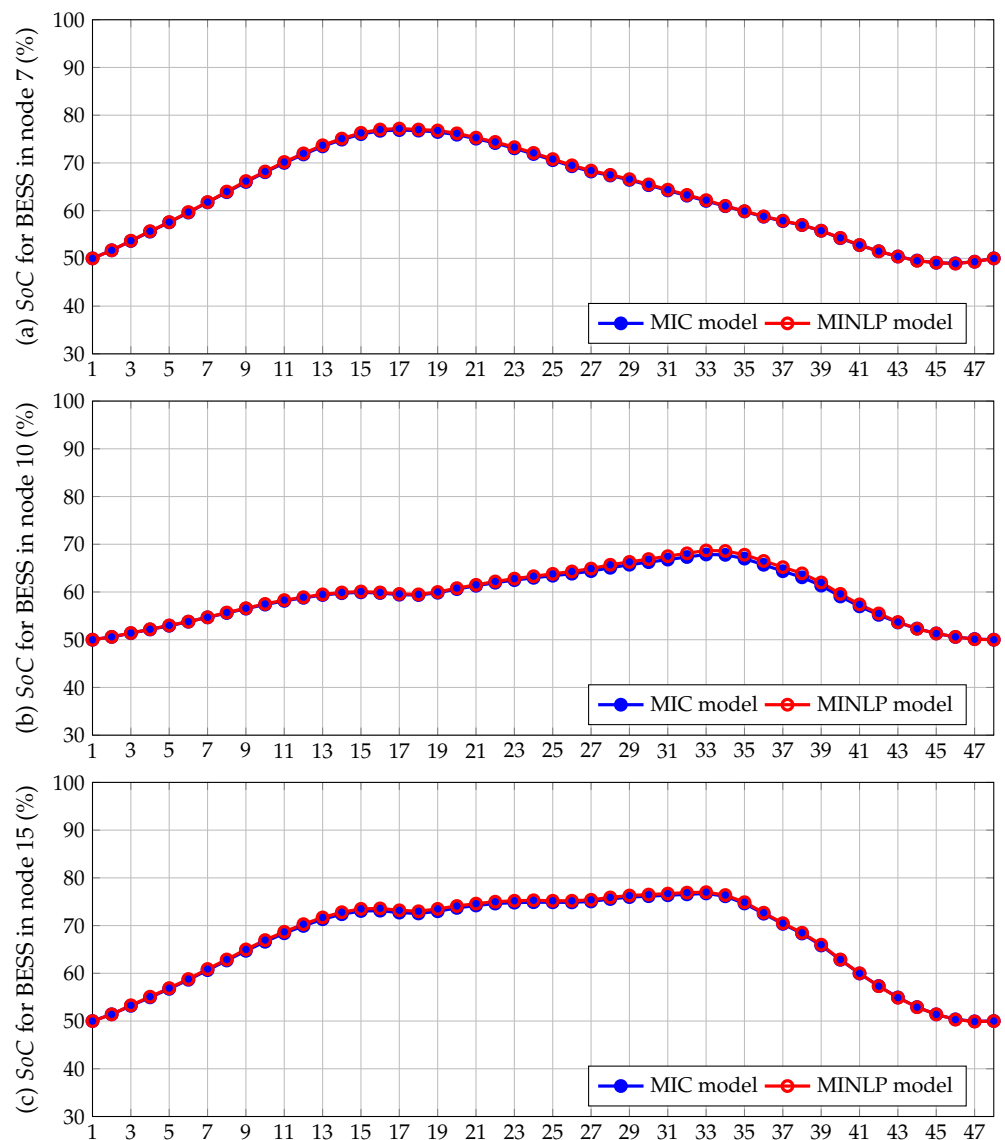| Model	BESS' Location	Generators' Location	Costs (COP$/Day)	Error (%)
MINLP	7 (A), 10 (B), 15 (B)	12 (Wind), 21 (PV)	52,957.92	0
MIC	7 (A), 10 (B), 15 (B)	12 (Wind), 21 (PV)	50,890.10	3.90

Figure 2. Comparison between exact the MINLP model and the proposed MIC model for Case 1:
(**a**) *SoC* for battery at node 7, (**b**) *SoC* for battery at node 10, and (**c**) *SoC* for battery at node 15.

6.2. Numerical Results for Case 2

In this simulation case, the original location of the renewable energy sources is fixed,
and the optimization model in Equations (1), (3)–(11), and (26) is implemented in the CVX
environment with the Gurobi solver in order to determine the best possible reallocation
sizes for the BESS. The numerical results of this simulation case are listed in Table 7. Note
that these locations are also set in the MINLP model in order to find the approximation
error of our proposal.

Table 7. Numerical results for the MIC and MINLP models in Case 2.

Model	BESS' Location	Generators' Location	Costs (COP$/Day)	Error (%)
MINLP	21 (A), 9 (B), 16 (B)	12 (Wind), 21 (PV)	41,847.61	0
MIC	21 (A), 9 (B), 16 (B)	12 (Wind), 21 (PV)	40,202.20	3.93

The numerical results in Table 7 show that the proposed convex model finds an
objective function value of COP$/day 40,202.20 by reallocating all the batteries to different
nodes with respect to the benchmark case. The new locations of the BESS are node 21

for the type A battery and nodes 9 and 16 for the type B batteries. Note that, when these new locations are fixed in the exact MINLP model, the final value of the objective function is COP$/day 41,847.61. The estimation error between both models is about 3.93%, which confirms the effective approximation made by the convex model to the exact optimization model.

Remark 3. *By comparing the solution values for the MINLP model in Cases 1 and 2, it is observed that the improvement of the objective function is about 11,110.31 Colombian pesos (COP) per day of operation, i.e., an improvement of 20.56% with respect to the benchmark case.*

6.3. Numerical Results for Case 3

In this simulation case, the locations of the batteries provided by the benchmark case are fixed (Table 3), and the proposed MIC model finds the optimal locations for the renewable energy sources. Once the convex model is solved, the new locations for the generators are set in the MINLP model in order to find the exact value of the objective function. All the numerical results for this scenario are listed in Table 8.

Table 8. Numerical results for the MIC and MINLP models in Case 3.

Model	BESS' Location	Generators' Location	Costs (COP$/Day)	Error (%)
MINLP	7 (A), 10 (B), 15 (B)	10 (Wind), 15 (PV)	29,697.73	0
MIC	7 (A), 10 (B), 15 (B)	10 (Wind), 15 (PV)	28,693.60	3.38

The numerical results in Table 8 show that the MIC model finds node 10 as the best location for the wind generators (originally at node 12) and node 15 for the PV source (originally at node 21), i.e., the generators must be moved to achieve a better performance regarding the objective function value. Note that this value, as approximated with the MIC model, was COP$/day 28,693.60. However, when the new locations of the generation sources were evaluated in the MINLP model, the final objective function value was COP$/day 29,697.73. These results imply an estimation error of 3.38%, thus confirming the efficiency of the proposed MIC model at approximating the exact solution of the studied problem.

Remark 4. *By comparing the solution values for the MINLP model in Cases 1 and 3, it is observed that the improvement of the objective function is about COP$/day 23260.19, i.e., an improvement of 43.33% with respect to the benchmark case. This result confirms that there is a better set of nodes to install all the renewable energy resources, with important contributions to the total costs of the energy losses per day of operation.*

6.4. Numerical Results for Case 4

This simulation scenario corresponds to the simultaneous allocation of BESS and renewable energy sources in the monopolar DC network while considering the recursive implementation illustrated in Algorithm 1. This simulation case starts by fixing the location of the renewable energy resources and finding the location of the batteries. Then, the location of the BESS is fixed, and the location of the renewable sources is found. This process is repeated until the location of BESS and the renewables remains unaltered, as this will be the optimal solution of the problem. The search process of the aforementioned methodology is listed in Table 9, along with its numerical results.

The numerical results in Table 9 show that, after four iterations, the location of the BESS and renewable energy sources is not further modified. The wind generator is assigned to node 10, the photovoltaic source to node 16, the type A battery to node 16, and the type B BESS to nodes 9 and 16. Note that the final objective function value at iterations 4 and 5 differs by about COP 5, even though the locations of the generators and the BESS are the same. This behavior is due to the fact that the model for iteration 4 determines the location

of the generators by fixing the BESS, while the model for iteration 5 fixes the location of the generators and determines the location of the BESS.

Table 9. Search process for the simultaneous allocation of BESS and renewables in monopolar DC networks using MIC models and recursive programming.

Iteration	Gen. Location	BESS' Location	Costs (COP$/Day)	Gen. Model	BESS' Model
1	Wind:12, PV:21	A:21, B:9, B:16	40,202.2		✓
2	Wind:11, PV:16	A:21, B:9, B:16	25,075.0	✓	
3	Wind:11, PV:16	A:16, B:9, B:12	24,438.5		✓
4	Wind:10, PV:16	A:16, B:9, B:12	23,993.2	✓	
5	Wind:10, PV:16	A:16, B:9, B:12	23,987.3		✓

Note that, in order to verify the efficiency of the proposed recursive model at locating renewables and batteries in monopolar DC networks, the final location of both devices (see row with iteration 5 in Table 9) is evaluated in the exact MINLP model to find the final exact value of the objective function. These results are listed in Table 10.

Table 10. Numerical results for the MIC and the MINLP models in Case 4.

Model	BESS' Location	Generators' location	Costs (COP$/Day)	Error (%)
MINLP	16 (A), 9 (B), 12 (B))	10 (PW), 16 (PV)	24,734.98	0
MIC	16 (A), 9 (B), 12 (B)	10 (PW), 16 (PV)	23,987.30	3.02

Note that the estimation error between the exact MINLP model and the proposed MIC model is just 3.02% regarding the final objective function values. This result confirms that the proposed convex model is efficient at solving problems regarding distributed energy resource allocation in monopolar DC networks.

Remark 5. *By comparing the solution values for the MINLP model in Cases 1 and 4, it is observed that the improvement of the objective function is about COP 28,222.94 per day of operation, i.e., an improvement of 53.29% with respect to the benchmark case. This result demonstrates that, for the 21-bus grid, there is a better combination of nodes to locate BESS and renewables than the benchmark case reported in [18].*

To illustrate the effectiveness of the MIC model at operating all the batteries in the 21-bus system, Figure 3 compares the daily operation of the batteries in nodes 9, 12, and 16. Notice that, as expected, all the batteries begin and end the day with 50% states of charge.

On the other hand, changes in the daily operation of the batteries between Cases 1 and 4 are also observed (compare Figures 2 and 3). Note, for example, that the batteries at nodes 9 and 12 now have state-of-charge peaks of 79.10 and 76.40% in simulation Case 4. In addition, starting at period of time 18, both batteries (Figure 3a,b) begin their discharging process. The most noticeable change is observed in Figure 3c. This battery is located in the same node as the photovoltaic source, and its state of charge and discharge is affected by it (location of the PV source), obtaining the maximum discharge in period 33, which was not observed in any of the graphs for the batteries presented in Figure 3. In addition, these graphs have a more pronounced behavior (higher slopes), which implies that the impact of the batteries on the DC network is even greater. This is why a reduction percentage of 53.29% was observed with respect to Case 1, which, in turn, demonstrates the effectiveness of the proposed model.
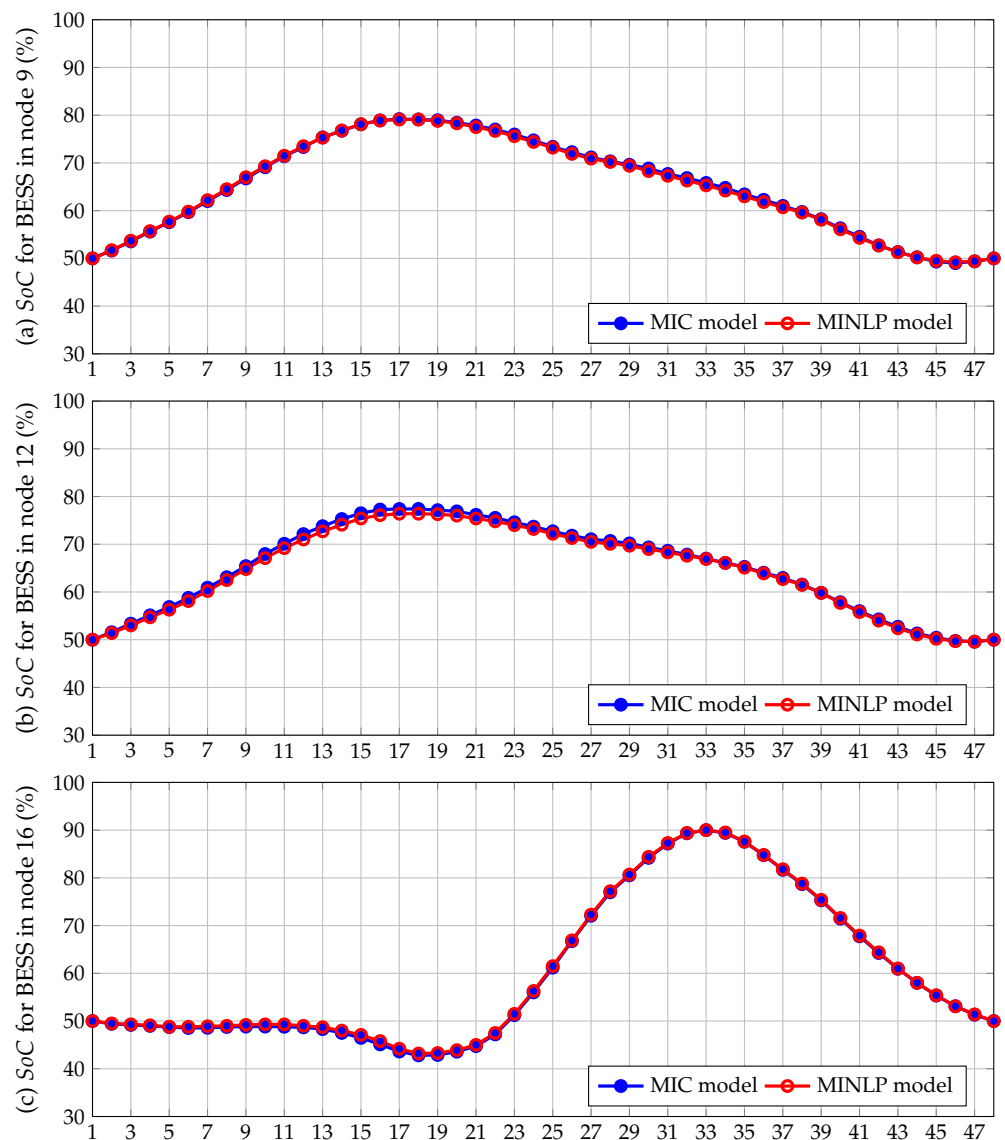
Figure 3. Comparison between the exact MINLP model and the proposed MIC one for Case 4: (**a**) *SoC* for battery at node 9, (**b**) *SoC* for battery at node 12, and (**c**) *SoC* for battery at node 16.

6.5. Summary of the Methodology

To illustrate the effect of placing the battery energy storage systems and the renewable energy resources on the objective function value, Figure 4 presents the daily behavior of the objective function for all the cases studied in the previous section.

Figure 4 presents the costs of the energy losses for all the cases considered regarding the location of BESS and renewable generators. Note that the area below each curve shows that the objective function is directly influenced by the position of the batteries and renewable energy sources. The main characteristic of the curves in Figure 4 is that the distributed energy resources can reduce the peak of the energy losses curves and flatten the curve, which is mainly associated with a better redistribution of the energy flow across the DC network due to the better locations of the distributed energy resources.
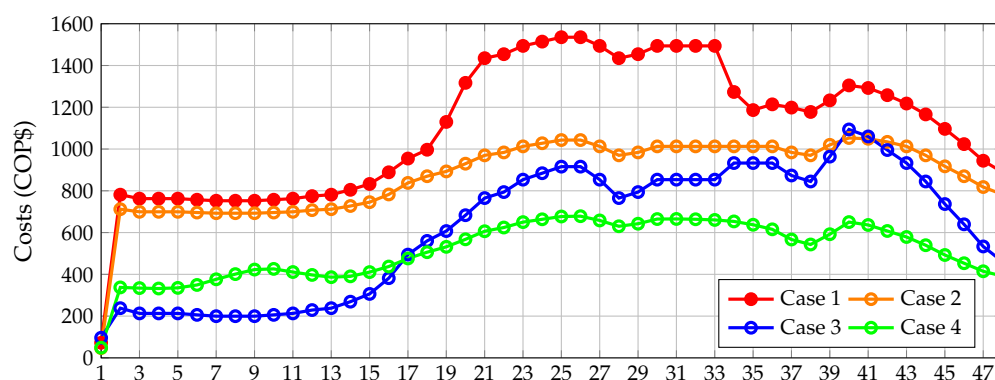
Figure 4. Daily behavior of the energy losses costs in the 21-bus grid as a function of the location of the distributed energy resources.

7. Conclusions and Future Work

This paper presented two MIC models for locating BESS and renewable energy sources in monopolar DC networks, which correspond to the convex approximations of the exact MINLP models for these problems. The main advantage of these formulations is that they ensure that the global optimum is found in MIC models by combining the Branch and Cut method with interior points, given the convexity of the solution space for each combination of binary variables. In addition, when the solution of the proposed MIC models was tested against the exact MINLP formulation, the estimation error of the objective function was lower than 4.0% in all simulation cases, which clearly confirms the effectiveness of the proposed models in solving the location of distributed energy resources for monopolar DC networks.

The following remarks can be made according to the numerical results of the four tested cases: (i) all the simulation cases show that, with respect to the benchmark case, there were improvements in the final expected daily energy losses costs; (ii) the best scenarios for objective function minimization where Cases 3 and 4, where renewable generators are located by fixing battery positions or both devices are simultaneously allocated (these results confirm that the higher impact on the final objective function is provided by the final location of the renewable energy source in the monopolar DC system); and (iii) the charging/discharging behavior of the BESS is highly influenced by their proximity to the renewable energy resources, since, when both devices are at the same node, the charging/discharging procedure does not contribute to additional energy losses because the energy interchange between both devices is performed in the same node without grid interaction.

Possible future works derived from this article can involve the following: (i) integrating the BESS model and the renewable energy location one into a unique mixed-integer convex model in order to non-iteratively solve the problem regarding the location of both devices, and (ii) proposing an improvement of the McCormick model to approximate the voltage profiles, using a recursive programming model that allows minimizing the estimation error of the objective function between the MINLP model and the MIC ones.

Author Contributions: Conceptualization, methodology, software, and writing (review and editing): J.D.B.-G., A.D.M.-C. and O.D.M. All authors have read and agreed to the published version of the manuscript.

References

1. Nandini, K.; Jayalakshmi, N.; Jadoun, V.K. An overview of DC Microgrid with DC distribution system for DC loads. *Mater. Today Proc.* **2022**, *51*, 635–639. [CrossRef]
2. Stieneker, M.; Doncker, R.W.D. Medium-voltage DC distribution grids in urban areas. In Proceedings of the 2016 IEEE 7th International Symposium on Power Electronics for Distributed Generation Systems (PEDG), Vancouver, BC, Canada, 27–30 June 2016; IEEE: Piscataway, NJ, USA, 2016. [CrossRef]
3. Montoya, O.D.; Serra, F.M.; Angelo, C.H.D. On the Efficiency in Electrical Networks with AC and DC Operation Technologies: A Comparative Study at the Distribution Stage. *Electronics* **2020**, *9*, 1352. [CrossRef]
4. Elattar, E.E.; Elsayed, S.K. Optimal Location and Sizing of Distributed Generators Based on Renewable Energy Sources Using Modified Moth Flame Optimization Technique. *IEEE Access* **2020**, *8*, 109625–109638. [CrossRef]
5. Paul, S.; Dey, T.; Saha, P.; Dey, S.; Sen, R. Review on the development scenario of renewable energy in different country. In Proceedings of the 2021 Innovations in Energy Management and Renewable Resources (52042), Kolkata, India, 5–7 February 2021; IEEE: Piscataway, NJ, USA, 2021. [CrossRef]
6. kumar Nath, U.; Sen, R. A Comparative Review on Renewable Energy Application, Difficulties and Future Prospect. In Proceedings of the 2021 Innovations in Energy Management and Renewable Resources (52042), Kolkata, India, 5–7 February 2021; IEEE: Piscataway, NJ, USA, 2021. [CrossRef]
7. Staffell, I.; Pfenninger, S. The increasing impact of weather on electricity supply and demand. *Energy* **2018**, *145*, 65–78. [CrossRef]
8. Dostál, Z.; Ladányi, L. Demands on energy storage for renewable power sources. *J. Energy Storage* **2018**, *18*, 250–255. [CrossRef]
9. Guerrero, J.; Blaabjerg, F.; Zhelev, T.; Hemmes, K.; Monmasson, E.; Jemei, S.; Comech, M.; Granadino, R.; Frau, J. Distributed Generation: Toward a New Energy Paradigm. *IEEE Ind. Electron. Mag.* **2010**, *4*, 52–64. [CrossRef]
10. Sibtain, D.; Murtaza, A.F.; Ahmed, N.; Sher, H.A.; Gulzar, M.M. Multi control adaptive fractional order PID control approach for PV/wind connected grid system. *Int. Trans. Electr. Energy Syst.* **2021**, *31*, e12809. [CrossRef]
11. Magaldi, G.L.; Serra, F.M.; de Angelo, C.H.; Montoya, O.D.; Giral-Ramírez, D.A. Voltage Regulation of an Isolated DC Microgrid with a Constant Power Load: A Passivity-Based Control Design. *Electronics* **2021**, *10*, 2085. [CrossRef]
12. Grisales, L.F.; Grajales, A.; Montoya, O.D.; Hincapie, R.A.; Granada, M.; Castro, C.A. Optimal location, sizing and operation of energy storage in distribution systems using multi-objective approach. *IEEE Lat. Am. Trans.* **2017**, *15*, 1084–1090. [CrossRef]
13. Gil-González, W.; Montoya, O.D.; Grisales-Noreña, L.F.; Cruz-Peragón, F.; Alcalá, G. Economic Dispatch of Renewable Generators and BESS in DC Microgrids Using Second-Order Cone Optimization. *Energies* **2020**, *13*, 1703. [CrossRef]
14. Akinyele, D.; Rayudu, R. Review of energy storage technologies for sustainable power networks. *Sustain. Energy Technol. Assess.* **2014**, *8*, 74–91. [CrossRef]
15. Shaqsi, A.Z.A.; Sopian, K.; Al-Hinai, A. Review of energy storage services, applications, limitations, and benefits. *Energy Rep.* **2020**, *6*, 288–306. [CrossRef]
16. Olabi, A.; Onumaegbu, C.; Wilberforce, T.; Ramadan, M.; Abdelkareem, M.A.; Alami, A.H.A. Critical review of energy storage systems. *Energy* **2021**, *214*, 118987. [CrossRef]
17. Karanja, J.M.; Hinga, P.K.; Ngoo, L.M.; Muriithi, C.M. Optimal Battery Location for Minimizing the Total Cost of Generation in a Power System. In Proceedings of the 2020 IEEE PES/IAS PowerAfrica, Nairobi, Kenya, 25–28 August 2020; IEEE: Piscataway, NJ, USA, 2020. [CrossRef]
18. Serra, F.M.; Montoya, O.D.; Alvarado-Barrios, L.; Álvarez-Arroyo, C.; Chamorro, H.R. On the Optimal Selection and Integration of Batteries in DC Grids through a Mixed-Integer Quadratic Convex Formulation. *Electronics* **2021**, *10*, 2339. [CrossRef]
19. Montoya, O.D. A convex OPF approximation for selecting the best candidate nodes for optimal location of power sources on DC resistive networks. *Eng. Sci. Technol. Int. J.* **2020**, *23*, 527–533. [CrossRef]
20. Wong, L.A.; Ramachandaramurthy, V.K. Optimal Allocation of Battery Energy Storage System Using Whale Optimization Algorithm. In Proceedings of the 2021 International Conference on Electrical, Computer, Communications and Mechatronics Engineering (ICECCME), Mauritius, Mauritius, 7–8 October 2021.

21. Home-Ortiz, J.M.; Pourakbari-Kasmaei, M.; Lehtonen, M.; Mantovani, J.R.S. Optimal location-allocation of storage devices and renewable-based DG in distribution systems. *Electr. Power Syst. Res.* **2019**, *172*, 11–21. [CrossRef]
22. Grisales-Noreña, L.; Montoya, O.D.; Ramos-Paja, C.A. An energy management system for optimal operation of BSS in DC distributed generation environments based on a parallel PSO algorithm. *J. Energy Storage* **2020**, *29*, 101488. [CrossRef]
23. Gil-González, W.; Montoya, O.D.; Holguín, E.; Garces, A.; Grisales-Noreña, L.F. Economic dispatch of energy storage systems in dc microgrids employing a semidefinite programming model. *J. Energy Storage* **2019**, *21*, 1–8. [CrossRef]
24. Kerdphol, T.; Tripathi, R.N.; Hanamoto, T.; Qudaih, Y.; Mitani, Y. ANN based optimized battery energy storage system size and loss analysis for distributed energy storage location in PV-microgrid. In Proceedings of the 2015 IEEE Innovative Smart Grid Technologies—Asia (ISGT ASIA), Bangkok, Thailand, 3–6 November 2015; IEEE: Piscataway, NJ, USA, 2015. [CrossRef]
25. Li, J.; Liu, F.; Wang, Z.; Low, S.H.; Mei, S. Optimal Power Flow in Stand-Alone DC Microgrids. *IEEE Trans. Power Syst.* **2018**, *33*, 5496–5506. [CrossRef]
26. Ploskas, N.; Sahinidis, N.V. Review and comparison of algorithms and software for mixed-integer derivative-free optimization. *J. Glob. Optim.* **2021**, *82*, 433–462. [CrossRef]
27. Torres, J.J.; Li, C.; Apap, R.M.; Grossmann, I.E. A Review on the Performance of Linear and Mixed Integer Two-Stage Stochastic Programming Software. *Algorithms* **2022**, *15*, 103. [CrossRef]
28. Garcés, A. On the Convergence of Newton's Method in Power Flow Studies for DC Microgrids. *IEEE Trans. Power Syst.* **2018**, *33*, 5770–5777. [CrossRef]